A Smart Bracelet Supporting Tactile Communication and Interaction

Stejara Dinulescu[1], Neeli Tummala[2], Gregory Reardon[1], Bharat Dandu[2], Dustin Goetz[3], Sven Topp[4], and Yon Visell[1,2,3]

***Abstract*— The sense of touch can convey semantic and emotional information in social or computer-mediated interactions. Touch plays an essential role in communication with individuals affected by multiple sensory loss, many of whom use modes of touch communication that can be broadly described as tactile sign languages. Few technologies exist today to support such interactions. Here, we present a smart bracelet for facilitating tactile communication and interaction. The smart bracelet captures and analyzes vibrations that are elicited in the skin via touch gestures performed on the hand. We demonstrate the utility of this system for supporting communication via the Deafblind Manual alphabet, which is a tactile sign language. This smart bracelet can classify signed letters with greater than 90% per-letter accuracy. These results show how existing modes of tactile communication can be integrated with information technologies. This work may furnish new paradigms for human-computer interaction via self- and interpersonal-touch contact.**

I. Introduction

The skin is a highly expressive medium used for perceiving and interacting with the world, including communication through touch. Indeed, touch interaction can convey significant meaning, intent, and sentiment. The diverse repertoire of touch interactions encountered in everyday settings, including interpersonal touch, contrasts starkly with the limited communicative and expressive range of touch found in most computing systems today. In some interpersonal interactions, including those involving individuals with multiple sensory impairments such as deafblindness, touch is the principal medium of communication [1], [2], [3]. Several languages, organizations, and educational systems exist to support the needs of individuals with deafblindness, but there exists a lack of accessibility for digital communication, which is crucial to address due to its ubiquity. However, current interaction paradigms primarily lie in the audiovisual domains. New technologies are needed that can enable individuals with all ranges of sensory abilities to engage with information technologies and digital resources.

Here, we present a smart bracelet for supporting tactile communication and interaction (Fig. 1A). This system captures vibration signals elicited in the skin by touch contact gestures performed on the hand; these gestures could be initiated by the wearer or by another person. The captured vibrations are analyzed using signal processing and machine learning methods that can recognize, from a designated lexicon, which gestures are performed (Fig. 1B1). We demonstrate the ability of this system to capture and classify touch gestures from the Deafblind Manual alphabet (Fig. 1C), a tactile sign language (TSL) used by individuals in Australia who are deafblind, in order to support digital tactile communication.

While several researchers have investigated *output* technologies for reproducing TSL [4], [5], [6], [7], the present work is, to the best of the authors' knowledge, the first *input device* specifically directed at supporting digital TSL communication. Such a device could address important unmet needs, such as those of transcribing information conveyed via TSL communications in court proceedings, emergencies, policy forums, scholarly meetings, or moments of personal or historical significance, especially where transcripts might otherwise be unavailable. Our TSL input device enables the letter-by-letter translation of touch gestures performed on the hand. One might, for example, use the palm of one's own hand to enter text, take notes, or send a text message normally requiring a standard phone interface (Fig. 1B2). Such a system could assist individuals with limited vision, for whom usage of mobile devices can be challenging.

In other applications, smart bracelets like the one presented here could also support the training of TSL interpreters. When combined with an output device capable of reproducing TSL gestures, such a smart bracelet could provide a means of TSL communication over the internet, including remote TSL interpretation, improving access to such services by many individuals. When combined with computer translation algorithms, such a smart bracelet could also facilitate conversation between individuals who communicate via different languages, including deafblind individuals who may not use the same TSL (Fig. 1B3). Indeed, a diverse variety of TSLs are used around the world [6].

A. Deafblindness and Tactile Communication

Research and development in automatic speech recognition and language processing over the past 50 years has yielded algorithms and systems for capturing, computationally understanding, and interacting with computers via speech. More recently, analogous methods to speech recognition have been used to support computer-based communication by detecting hand poses during visual sign languages, such as American Sign Language [8]. To

[1]Stejara Dinulescu, Gregory Reardon, and Yon Visell are with the Department of Media Arts and Technology, University of California, Santa Barbara, Santa Barbara, CA 93106 sdinulescu@ucsb.edu

[2]Neeli Tummala, Bharat Dandu, and Yon Visell are with the Department of Electrical and Computer Engineering, University of California, Santa Barbara, Santa Barbara, CA 93106

[3]Dustin Goetz and Yon Visell (by courtesy) are with the Department of Mechanical Engineering, University of California, Santa Barbara, Santa Barbara, CA 93106

[4]Sven Topp is with the School of Psychology, University of Sydney, Camperdown NSW 2006, Sydney, Australia

2022 IEEE Haptics Symposium (HAPTICS) | 978-1-6654-2029-7/22/$31.00 ©2022 IEEE | DOI: 10.1109/HAPTICS52432.2022.9765616

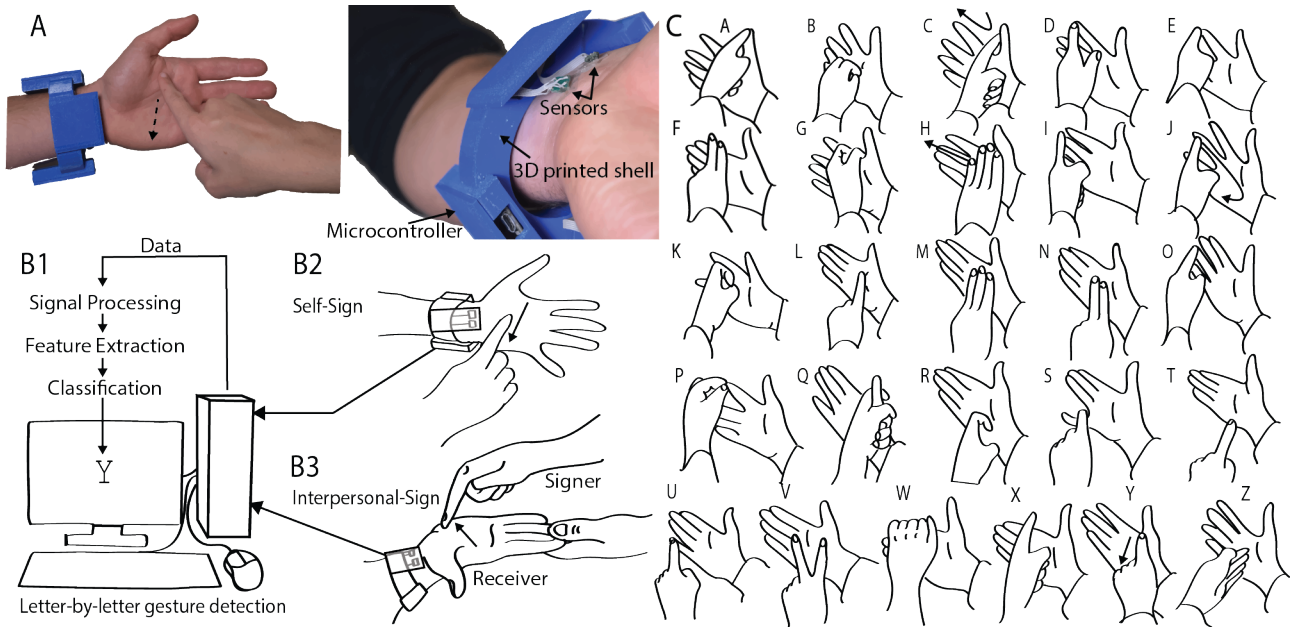

Fig. 1. A) Wrist-worn acoustic sensing interface to encode and detect touch gestures on the hand. B) System overview and envisioned applications for detection of touch gestures on the skin. B1) Touch signals signed on the palm are transmitted to a PC via serial communication with the microcontroller. The data is processed and features are extracted to be used for classification. B2) Wearable interface enables self-signing on the palm of the hand to encode semantic meaning for note-taking purposes, sending a remote text message via touch, or transcription/record-keeping in the tactile domain. B3) Wearable interface translates interpersonal touch gestures as they are being signed. This could facilitate learning of TSL gestures, transcription of conversations in the tactile domain, and translation of TSL in real-time when the wearer is uncertain of the semantic mappings of the alphabet. C) The 26 letters of the Deafblind Manual alphabet.

date, little attention has been given to achieving similar goals in tactile communication, particularly TSLs.

A recent report by the World Federation of the Deafblind indicates that between 0.2-2% of people are impacted by sensory impairment of both vision and hearing. Deafblind individuals use a variety of languages for tactile communication, depending on their region, community, and individual factors, such as the onset and severity of sensory impairment. Many TSLs exist today supporting critical daily activities and social interaction [9]; in addition, many of the TSLs are letter-based semantic touch communication methods. Here, we demonstrate a system for supporting TSL communication, specifically utilizing the Deafblind Manual alphabet, which involves the performance of touch gestures, including tapping, lightly pinching, and sliding on the surface of the hand. Each of the 26 gesture patterns corresponds to a letter in the English alphabet [6] (Fig. 1C).

Other technologies for supporting communication by individuals with visual and auditory sensory loss include Braille interfaces, emerging methods for tactile graphic displays, and more commonly available screen-based accessibility features for those with low vision. However, such methods do not support the communication needs of all individuals who are deafblind. More recently, researchers have engineered systems to translate text or speech into tactile patterns [4], [5], including TSL gestures [6], [9], [10]. However, the authors are not aware of any prior efforts to facilitate or develop a computational encoding of tactile input. A system such as the one presented here could support TSL communication by enabling transcription, analysis, or reproduction of TSL interactions.

B. Capturing Touch Gestures via Vibration Signatures

Touch interactions with the skin elicit vibrations that travel far from the point of contact, encoding information about the contact location and nature of the gesture [11], [12], [13], [14], [15]. This physical process makes it feasible to collect information about tactile interactions using vibration sensors that are positioned remotely from the contact location. Human-computer interaction research has utilized such processes to provide means of computational input via contact with the skin, as in the Skinput device [16]. Many other sensing methods can be used for capturing information from skin contact, including capacitive, electromyography, ultrasound, force, and other sensing techniques [17], [18], [19], [20]. However, the propensity of touch-elicited vibrations to travel great distances in the skin and the efficiency with which such signals can be captured electronically via low-cost, readily available sensors makes this approach particularly attractive for interactive device engineering, especially in settings where it is preferable to leave the hand unencumbered.

C. Summary of Contributions

We present a smart wrist wearable for capturing and recognizing touch gestures that occur on the hand during skin-to-skin contact. To inform the design of this smart bracelet, including the number and placement of sensors, we captured the signal profiles of a subset of letters of the Deafblind Manual alphabet with high spatial resolution using

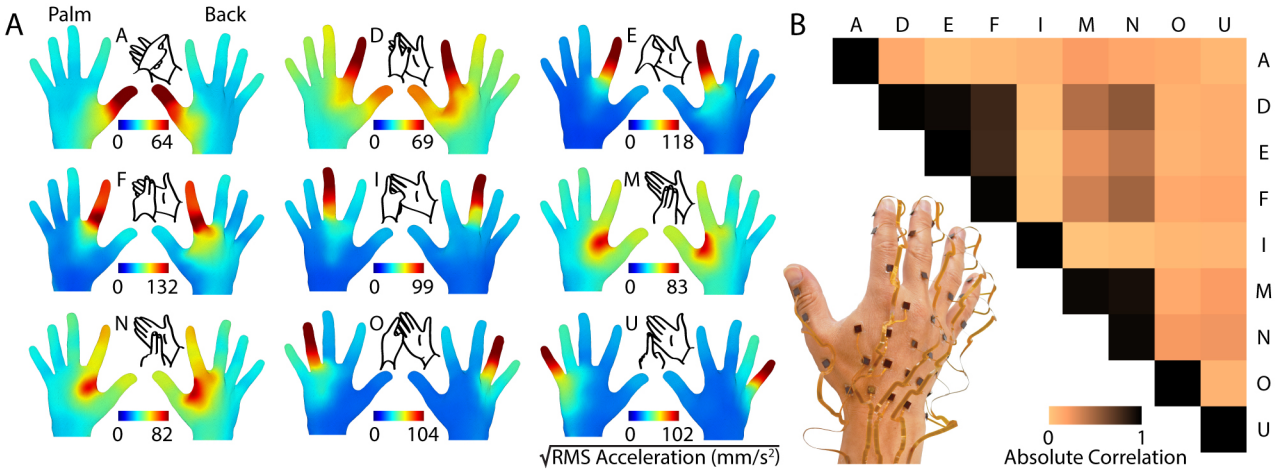

Fig. 2. A) Measured whole-hand mechanical responses for a subset of the Deafblind Manual alphabet. We found that the contact is not only reflected in skin responses at the touched location, but also that this energy propagated outwards to regions on the skin, on both sides of the hand, far from the point of contact. B) We found that the tactile gestures produced consistent, repeatable patterns of RMS acceleration across the hand (mean absolute correlation > 0.95 within trials of the same gesture), while yielding very low correlations when comparing across trials of different gestures.

a sensor array encompassing the whole hand. By analyzing this data, we identified that even letters that are highly similar to one another in tactile sign contain unique signal profiles, even when measured at locations removed from the gesture contact. Informed by this finding, we designed a compact, wrist-worn device to capture these propagating signals without hindering natural manual movements and tactile interactions. To demonstrate the utility of this system for tactile communication, we illustrate the capacity of our device to classify 26 different touch gestures—in this case, the letters of the Deafblind Manual alphabet. We find that the device can accurately discriminate between different touched contact locations (e.g. digit II, digit V, or palm) and between different types of touch contact (e.g. slides, impulses, pinches, or squeezes). We show using simple, supervised machine learning methods that such a device is able to identify these 26 different gestures with above 90% accuracy, even when trained on a small dataset.

II. Whole-Hand Sensing

A. Materials and Methods

In a first experiment, we surveyed the whole-hand mechanical responses produced during the signing of a subset of letters from the Deafblind Manual alphabet. We used two 42-channel, 3-axis accelerometer arrays (Model LI3DSH, ST Microelectronics) [12]. We captured data at a rate of 1300 Hz via a field-programmable gate array (FPGA) based multichannel data acquisition board, with firmware on the FPGA and software on a Windows PC. We affixed each accelerometer in the array to the skin via doubled-sided adhesive, with one array attached to the dorsal side of the hand and the other to the palmar (Fig. 2B).

We captured the skin acceleration for 10 trials of 9 letters of the Deafblind Manual alphabet (A, D, E, F, I, M, N, O, U), signed on the palmar side of the hand through interpersonal touch (i.e one person signs on the hand of another person). Letters were chosen for high frequency of use (i.e. vowels) and letter similarity (i.e. M and N, D and E). Because the palmar surface of the hand was also covered with sensors, we slightly shifted the signed location of M and N to avoid interfering with the sensors. The palm was held facing upwards, with the forearm stabilized against the edge of a table at chest-level to minimize noise from spurious hand movements. The data consisted of ten, 84-channel 3-axis acceleration signals for each letter. The data was de-meaned and bandpass filtered, then compressed to a single axis by computing the magnitude of the vector. We then computed the RMS of the acceleration magnitude.

To determine the spatial distribution of acceleration energy for each gesture class, we compute root mean square (RMS) acceleration over all trials. We interpolated these data using coordinates obtained from an anatomically plausible 3D hand model using squared distance weighting. We analyzed the differences between letters using this data and also computed the mean pairwise absolute correlation (Pearson's r) between the RMS acceleration of all trials and of all letters.

B. Results

Each tactile gesture class yielded distributions of RMS acceleration that reflected the contact location and the nature of the gesture (single touch - A, E, I, O, U and multi-touch - D, F, M, N) (Fig. 2A). For example, the peak RMS acceleration of the letter E was localized to the point of contact. Multi-touch gestures tended to deliver high RMS acceleration (relative to the peak RMS acceleration for that gesture) to locations far from the point of contact, reflecting that the contact location on the hand was much larger (2-3 times the size of the contact for single touch gestures). Furthermore, all gestures delivered energy to the wrist; the amount of RMS acceleration delivered at the wrist was a function of the distance from the contact location (e.g. the contact location for E is much further from the wrist than for M/N).

978-1-6654-2029-7/22/$31.00 ©2022 IEEE

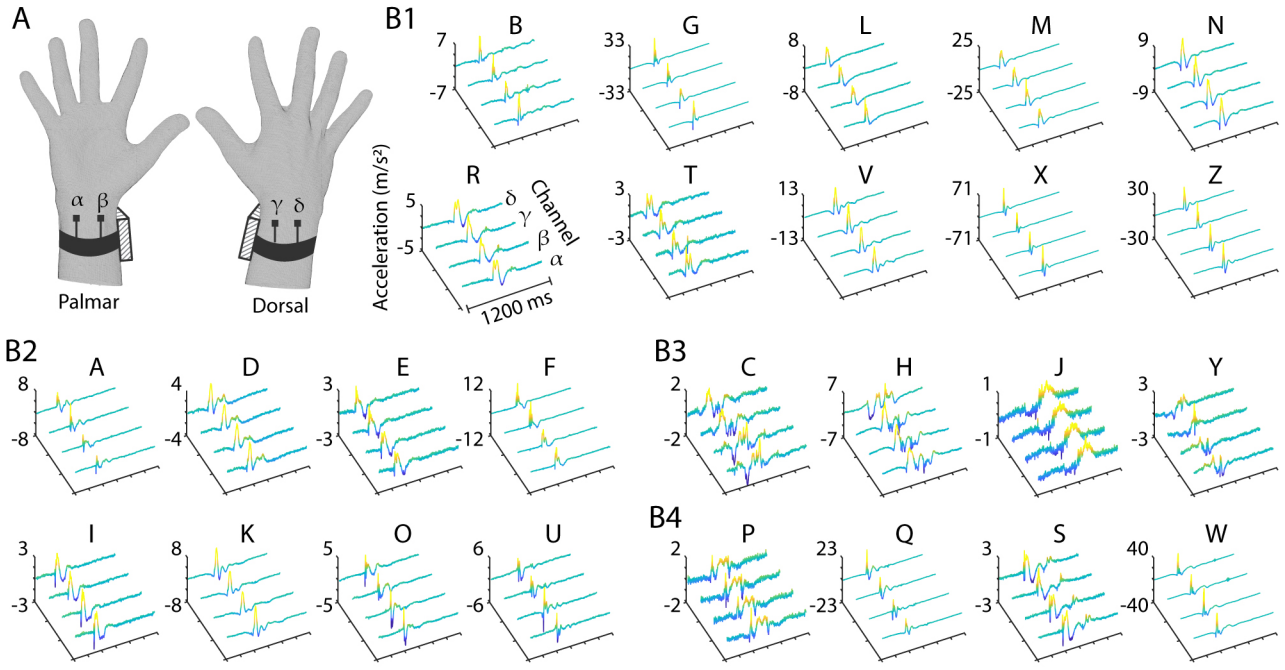

Fig. 3. A) Wrist-wearable device using four accelerometers affixed to the skin to capture mechanical vibrations produced during tactile fingerspelling. B) Measured accelerometer signals produced during a single trial of each letter of Deafblind Manual alphabet. Palm tap and finger tap gestures (B1 and B2, respectively) produced transients that rapidly decayed. Finger taps tended to deliver less energy to the wrist when compared to palm taps, reflecting the difference in distance between the point of contact and the sensor. Sliding or pinching/grabbing gestures (B3 and B4, respectively) produced signals that tended to decay at a much slower rate on the skin, reflecting that the gesture occurs over a longer time scale than the tap gestures.

The tactile gestures elicited vibration patterns that were consistent across gesture instances (Fig. 2B), and were qualitatively distinct from the other gestures. Consistent with the observations of the whole-hand patterns (Fig. 2A), some gestures produced similar distributions of RMS acceleration and thereby high correlations (i.e. M/N and D/E/F). For the subset of data captured by the ten accelerometers located on the wrist, averaged within-gesture mean absolute correlations of the RMS acceleration (0.94) were substantially larger than across-gesture correlations (0.48). These results suggested that acceleration information captured at the wrist could be used to classify varied tactile gestures.

III. Wrist-Worn Interface

Informed by the preceding findings, including the extent to which similar information could be captured via sensors at locations removed from the point of contact with the hand, we designed a smart bracelet using a minimal arrangement of sensors located at the wrist. We evaluated the utility of this device for classifying touch contact gestures performed on the hand, in the form of TSL gestures.

A. Materials and Methods

1) Device Design: The device was composed of an ABS shell enclosing two Adafruit Feather M0 WiFi microcontrollers. It employed a total of four 3-axis analog accelerometers (Analog Devices ADXL335) (Fig. 1A). Each sensor was adhered to the skin. Pairs of sensors were positioned 25 mm apart on both the palmar and dorsal sides of the wrist (Fig. 3A), at locations determined from the preceding experiment. The casing for the electronics was designed to avoid mechanically disturbing the sensing elements. The data was captured at a sampling frequency of 1250 Hz and at a resolution of 12 bits using the onboard ADC of the microcontroller.

2) Collection of TSL Data: We collected accelerometer measurements during TSL touch contact in each of two conditions: one in which the signer performed gestures on their own hand (self-sign, or SS, depicted in Fig. 1B2) and one in which the signer contacts another person's hand (interpersonal-sign, or IS, depicted in Fig. 1B3). The palmar surface of the hand, held outstretched and flat, was facing upwards throughout data collection, with the dorsal side of the forearm stabilized against the edge of a table to minimize disturbance from unintentional limb movements. In both conditions, we recorded 40 trials of each of the 26 letters.

3) Signal Processing and Feature Extraction: The data for each letter were segmented, lowpass filtered at 250 Hz, and compressed from 3 axes to 1 axis using principal component analysis (PCA). After compression, the data for each trial was normalized independently,

$$y_{c,n} = \frac{y_{c,n}}{\max_{\{c,n\}} |y_{c,n}|} \quad (1)$$

where n is the sample number and c is the channel number. This preserved the inter-channel differences between accelerometers, while also reducing inter-trial variability of the same gesture and improving the consistency of the feature estimates across gestures.

For every trial, we computed time-domain, frequency-

domain, and spectro-temporal features for all 4 channels of each analyzed segment, yielding 96 features per trial. The time-domain features were peak-to-peak amplitude

$$PTP_c = |\max_n y_{c,n} - \min_n y_{c,n}| \tag{2}$$

and mean absolute deviation

$$MAD_c = \frac{1}{N}\sum_{n=1}^{N} |y_{c,n} - \bar{y}_c| \tag{3}$$

where $\bar{y}_c$ is the mean of signal $y_{c,n}$. This yielded a total of 8 time-domain features per segment.

For the second set of features, we computed the Discrete Fourier Transform (DFT) of each of the normalized signals, $Y_{c,k} = \mathcal{F}\{y_{c,n}\}$, where $\mathcal{F}$ is the DFT. From the frequency-domain representation of the signal, we computed the spectral centroid

$$SC_c = \frac{\sum_{k=1}^{N} f_k |Y_{c,k}|}{\sum_{k=1}^{N} |Y_{c,k}|} \tag{4}$$

where f_k is the center frequency of bin k and $|Y_{c,k}|$ is the magnitude of bin k for channel c. In addition, we computed the center frequency of the DFT bin with the largest magnitude for each channel c,

$$F_c = f_{k^*} \text{ s.t. } k^* = \arg\max_k |Y_{c,k}| \tag{5}$$

We computed the mean and standard deviation of the DFT bins over a 50 Hz bandwidth. Let the bandwidth $b_i \in \{[0\ 50], [50\ 100], [100\ 150], [150\ 200], [200\ 250]\}$ for $i = 1, ..., 5$. We associate the set of bins K_i whose center frequencies lie within bandwidth b_i and compute:

$$\mu_{c,b_i} = \frac{1}{|K_i|}\sum_{k \in K_i} |Y_{c,k}| \quad , \tag{6}$$

$$\sigma_{c,b_i} = \sqrt{\frac{1}{|K_i|}\sum_{k \in K_i} (|Y_{c,k}| - \mu_{c,b_i})^2} \tag{7}$$

where $|K_i|$ is the size of set K_i. This produced 40 features (2 measures $\times$ 5 bandwidths $\times$ 4 channels), for a total of 48 frequency-domain features.

Finally, we composed a set of spectro-temporal features to capture temporal variations in the spectral envelope of the signal. We computed the Short-Time Fourier Transform (STFT) of the signals (window size K=256 samples, 50% overlap, Hanning window), yielding a matrix of Fourier coefficients ($M \times K$) for each channel c where each of the M rows is the DFT of the signal over different times. We computed the mean and standard deviation of the measure μ_{c,b_i} (see Eq. 6) for each row of the Fourier matrix. Let $\mu_{c,b_i,m}$ be the mean of bandwidth b_i for channel c for row m. We compute

$$\mu^{STFT}_{c,b_i} = \frac{1}{M}\sum_{m=1}^{M} \mu_{c,b_i,m} \quad , \tag{8}$$

$$\sigma^{STFT}_{c,b_i} = \sqrt{\frac{1}{M}\sum_{m=1}^{M} (\mu_{c,b_i,m} - \mu^{STFT}_{c,b_i})^2} \tag{9}$$

This yielded another set of 40 features (2 measures $\times$ 5 bandwidths $\times$ 4 channels). All features (temporal, frequency, and spectro-temporal) were concatenated to form a 96-dimensional vector, used to train the machine learning model and classify the 26 different tactile gestures.

4) TSL Classification: To distinguish the 26 letters of the Deafblind Manual alphabet via our smart bracelet, we pass computed features into three common supervised machine learning classification models: a support vector machine with a linear kernel (SVM), logistic regression with PCA (LR), and a random forest model (RF). To minimize bias during training and classification, we employed a 10-fold cross-validation procedure with a 90-10 train-test split. During each classification run, we computed the mean and variance of each feature in the training data and used these sample moments to whiten both the training and testing data. We performed classification for each mechanical dataset separately (SS and IS conditions, 40 trials per letter) and on both datasets (combined condition, 80 trials per letter).

B. Results and Discussion

1) Mechanical Signal Profiles: We found that the measured signals (Fig. 3B) yielded noticeably different time-domain acceleration responses, which became more prominent when we grouped the gestures by palm taps (Fig. 3B1), finger taps (Fig. 3B2), slides (Fig. 3B3), and pinches/grabs (Fig. 3B4). We found that tapping gestures yielded transient signals that decayed rapidly, while slides and pinches/grabs decayed at much slower rates in the skin. This likely reflects the variation in contact conditions between the gestures, for which slides and pinches/grabs occur at much longer time scales. We found that finger taps delivered less energy to the wrist when compared to palm taps, reflecting that the properties of the skin, which is a highly damped medium, play a role in encoding the distance from the contact location to the wrist, thereby differentiating the measured tactile gestures. Finally, we found that sliding gestures, regardless of contact location, tended to deliver less energy to the wrist, but that this energy was nonetheless measurable and informative.

2) TSL Classification: When utilizing data from all four sensors, the SVM classifier consistently outperformed the RF and LR classifiers in the SS and IS conditions, with average accuracies greater than 93% across cross-validation folds; in the combined condition, the RF classifier slightly outperformed the others at close to 90% average accuracy across folds (Table I). High performance using SVM is promising for real-time applications, as a trained SVM model can easily be implemented on a micro-controller without the need for additional computational power. In the following analysis, we focus on the performance of the SVM model.

We further analyzed classification performance using different subsets of sensor channels (Fig. 3A) to determine the minimal number of sensing element required for robust classification. The subsets considered include all four channels ($\alpha, \beta, \gamma, \delta$), two channels on the palmar side of the wrist (α, β), two channels on the dorsal side of the wrist (γ, δ), one channel on the palmar side of the wrist

	Classifier		
Dataset	SVM	RF	LR
SS	93.9	88.7	90.6
IS	93.7	92.2	91.0
Combined	86.3	89.4	76.1

TABLE I
AVERAGE CLASSIFICATION ACCURACY (%) ACROSS DATASETS AND MODELS FOR 4-SENSOR CONFIGURATION

	Sensor Configuration					
Dataset	$\alpha, \beta, \gamma, \delta$	α, β	γ, δ	α, γ	α	γ
SS	93.9	86.5	86.8	87.1	76.3	73.8
IS	93.7	88.3	85.4	87.1	75.0	75.4
Combined	86.3	76.8	75.6	78.4	61.6	64.3

TABLE II
AVERAGE CLASSIFICATION ACCURACY (%) ACROSS DATASETS AND SENSOR CONFIGURATIONS FOR SVM MODEL

(α), and one channel on the dorsal side of the wrist (γ). Table II summarizes the average classification accuracies across cross-validation folds for the SS, IS, and combined datasets. The use of all four channels yields the highest classification accuracies, but the employment of just two sensors maintains robust performance (above 85% in the single subject conditions), indicating that they are sufficient for detecting various sets of tactile gestures. Mounting the sensors on the palmar or dorsal side of the wrist does not significantly change classification accuracies. On the other hand, classification accuracy drops significantly when using only one sensor, indicating that inter-channel differences encode relevant classification information that cannot be discarded. Close inspection of the signals shown in Fig. 3B shows differences in the phase and shape of signals between channels, most evident in the sliding gestures.

We found that the most commonly misclassified letters were L and N, which is expected due to the similarity of the tactile gestures; N is signed with two fingers in the center of the palm whereas L is signed with one finger in the same location (Fig. 4). Additionally, R and T are commonly mislabeled, as they are both taps occuring near the same palmar location: T with one finger and R with two fingers. Other commonly misclassified letter pairs include G and X, and W and Z. The former are gestures performed with the signer's whole hand, producing high acceleration signals at the palm; the latter produce similar high energy signals, but occur at different locations on the hand.

We also examined classification accuracy within each gesture grouping shown in Fig. 3B (i.e. palm taps, finger taps, slides, and pinches/grabs) for the combined dataset in the four channel configuration, averaged across cross-validation folds. Sliding gestures are classified with the highest accuracy (92.8%), likely because they produce the most distinct mechanical signals. Finger taps are also accurately classified (90.8% accuracy) and are generally only misclassified as other finger taps, likely because the captured signals often possess similar magnitudes and temporal profiles. Similarly, palm taps (81.1% accuracy) are accurately recognized and are typically only misclassified as other palm taps. This

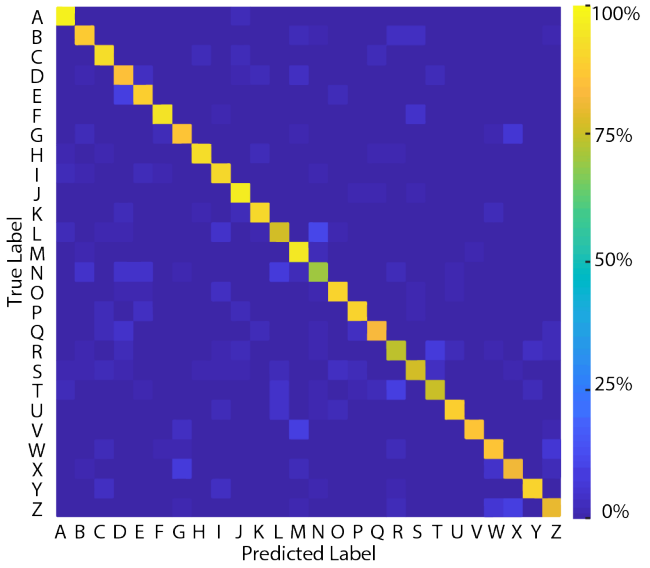

Fig. 4. Confusion matrix for the linear SVM Classifier on the combined dataset, with per-letter accuracies along the diagonal. On the off-diagonal, type I (false positives) read column-wise and type II (false negatives) read row-wise. Commonly misclassified letter pairs can often be grouped into the subsets introduced in Fig. 3. For example. {E,D} are both taps on digit II, and {G, X, Z}, {L, N}, and {R, T} are all taps on the palm.

is expected when considering the similarity between many of the palm taps; for example, L, M, N, and V are all signed in the middle of the palm but with different finger placements. Finally, pinch or grab gestures (83.8% accuracy) are somewhat more likely to be misclassified as other types of gestures due to their heterogeneous nature.

Regardless of the classifier, dataset, or sensor configuration, we observe accuracies above 60%, which is significantly higher than chance (3.9% for 26 classes). In the majority of SS and IS conditions, accuracies are above 90% when using four sensors, regardless of classifier used. This indicates that accuracies approaching 100% can likely be achieved via standard techniques such as lexicon-based models that are widely used in natural language processing and automatic speech recognition. Further improvements might also be achieved through the use of state-of-the-art multi-layer neural network classifiers.

IV. CONCLUSION

We present a smart bracelet system that transforms the skin into a touch gesture input interface. The bracelet can classify touch gestures of the Deafblind Manual alphabet, via integrated wrist-worn sensors, with significantly higher-than-chance accuracy. Our approach demonstrates the success of minimal accelerometer-based sensing that leaves the hand unencumbered for manual interactions and movements. Measurements from a whole-hand sensing array were used in an initial exploration to identify a subset of four sensors that are able to capture enough salient information in a touch gesture, thus reducing cost and complexity. We demonstrated the utility of this device for supporting tactile communication via TSL. We present analyses of an experiment in which we cap-

tured and accurately classified signal profiles for all 26 letters of the Deafblind Manual alphabet, demonstrating promising uses of such systems for supporting tactile communication.

The smart bracelet can be used for input via tactile gestures performed on the hand of the user by the user, which could be useful for note-taking, transcription, or textual communication. Such a device could support interpersonal tactile communication by individuals who prefer using touch over other modalities, in addition to encoding touch in the digital domain. These findings may also enhance the utility of output devices for tactile communication. Utilizing input and output devices in conjunction could support communication between two or more individuals, including people who may communicate via different TSLs.

While we have demonstrated the capability to accurately classify the 26 gestures of the Deafblind Manual alphabet, more remains to generalize features for classification of larger mechanical datasets consisting of various TSL signers, receivers, and alphabets. Further investigation into individual differences between subjects, such as hand size, signing speeds, and emotion (i.e. happy, angry) conveyed through TSL, will be experimentally investigated.

We further envision supporting real-time classification of TSL, where signing occurs as fast as five letters per second [6]. In these cases, intentional or accidental movements of the hand (such as finger motion from a previously performed tactile gesture) must not interfere with signals captured from the sensors. Thus, further data capture and signal processing methods will be explored, examples of which include capturing data from two devices worn on both the signer's and receiver's wrist, or capturing false positive dataset examples (such as muscle contractions, finger twitches, etc.) to help identify gestural noise versus salient gesture data. We will additionally explore multi-layer classification and feature optimization by additional meta-analysis of similarities and differences between tactile signals in a gesture set, as well as natural language processing as previously applied in speech technologies. Such advancements are expected to improve accuracy and robustness, aiding applications in natural communication. This system holds promise for supporting tactile communication, including scenarios where it is paired with a haptic communication output device, to address communication needs of individuals who are deafblind.

ACKNOWLEDGMENT

The authors thank Basil Duvernoy, Jeraldine Milroy, and Yitian Shao for their feedback. The authors acknowledge support from the University of California, Office of the President, National Science Foundation (NSF) Fellowship No. 2139319 to Dinulescu and Goetz, and NSF award 1751348 to Visell. Any opinion, findings, and conclusions or recommendations expressed in this material are those of the authors and do not necessarily reflect the views of the NSF.

REFERENCES

[1] C. M. Reed, W. M. Rabinowitz, N. I. Durlach, L. D. Braida, S. Conway-Fithian, and M. C. Schultz. Research on the tadoma method of speech communication. *The Journal of the Acoustical Society of America*, 77(1):247–257, 1985.

[2] C. M. Reed, L. A. Delhorne, and N. I. Durlach. Tactile reception of fingerspelling and sign language. *The Journal of the Acoustical Society of America*, 82(S1):S24–S24, 1987.

[3] Jack M. Loomis. On the tangibility of letters and braille. *Perception & Psychophysics*, 29(1):37–46, January 1981.

[4] Hugo Nicolau, Kyle Montague, Tiago Guerreiro, André Rodrigues, and Vicki L Hanson. Holibraille: Multipoint vibrotactile feedback on mobile devices. In *Proceedings of the 12th International Web for All Conference*, pages 1–4, 2015.

[5] Ulrike Gollner, Tom Bieling, and Gesche Joost. Mobile lorm glove: introducing a communication device for deaf-blind people. In *Proceedings of the sixth international conference on tangible, embedded and embodied interaction*, pages 127–130, 2012.

[6] Basil Duvernoy, Ildar Farkhatdinov, Sven Topp, and Vincent Hayward. Electromagnetic actuator for tactile communication. In *International Conference on Human Haptic Sensing and Touch Enabled Computer Applications*, pages 14–24. Springer, 2018.

[7] Hong Z. Tan, Charlotte M. Reed, Yang Jiao, Zachary D. Perez, E. Courtenay Wilson, Jaehong Jung, Juan S. Martinez, and Frederico M. Severgnini. Acquisition of 500 english words through a tactile phonemic sleeve (taps). *IEEE Transactions on Haptics*, 13(4):745–760, 2020.

[8] C. Vogler and D. Metaxas. Parallel hidden markov models for american sign language recognition. In *Proceedings of the Seventh IEEE International Conference on Computer Vision*, volume 1, pages 116–122 vol.1, 1999.

[9] Basil Duvernoy, Sven Topp, and Vincent Hayward. Hapticomm, a haptic communicator device for deafblind communication. In *International AsiaHaptics conference*, pages 112–115. Springer, 2018.

[10] Arthur Theil, Lea Buchweitz, James Gay, Eva Lindell, Li Guo, Nils-Krister Persson, and Oliver Korn. Tactile board: A multimodal augmentative and alternative communication device for individuals with deafblindness. In *19th International Conference on Mobile and Ubiquitous Multimedia*, MUM 2020, page 223–228, New York, NY, USA, 2020. Association for Computing Machinery.

[11] Yitian Shao, Vincent Hayward, and Yon Visell. Spatial patterns of cutaneous vibration during whole-hand haptic interactions. *Proceedings of the National Academy of Sciences*, 113(15):4188–4193, 2016.

[12] Yitian Shao, Hui Hu, and Yon Visell. A wearable tactile sensor array for large area remote vibration sensing in the hand. *arXiv preprint arXiv:1908.08199*, 2019.

[13] Yitian Shao, Vincent Hayward, and Yon Visell. Compression of dynamic tactile information in the human hand. *Science advances*, 6(16):eaaz1158, 2020.

[14] Xavier Libouton, Olivier Barbier, Yorick Berger, Leon Plaghki, and Jean-Louis Thonnard. Tactile roughness discrimination of the finger pad relies primarily on vibration sensitive afferents not necessarily located in the hand. *Behavioural brain research*, 229(1):273–279, 2012.

[15] Katherine O Sofia and Lynette Jones. Mechanical and psychophysical studies of surface wave propagation during vibrotactile stimulation. *IEEE transactions on haptics*, 6(3):320–329, 2013.

[16] Chris Harrison, Desney Tan, and Dan Morris. Skinput: appropriating the skin as an interactive canvas. *Communications of the ACM*, 54(8):111–118, 2011.

[17] Adiyan Mujibiya, Xiang Cao, Desney S Tan, Dan Morris, Shwetak N Patel, and Jun Rekimoto. The sound of touch: on-body touch and gesture sensing based on transdermal ultrasound propagation. In *Proceedings of the 2013 ACM international conference on Interactive tabletops and surfaces*, pages 189–198, 2013.

[18] Yang Zhang, Wolf Kienzle, Yanjun Ma, Shiu S Ng, Hrvoje Benko, and Chris Harrison. Actitouch: Robust touch detection for on-skin ar/vr interfaces. In *Proceedings of the 32nd Annual ACM Symposium on User Interface Software and Technology*, pages 1151–1159, 2019.

[19] Subramanian Sundaram, Petr Kellnhofer, Yunzhu Li, Jun-Yan Zhu, Antonio Torralba, and Wojciech Matusik. Learning the signatures of the human grasp using a scalable tactile glove. *Nature*, 569(7758):698–702, 2019.

[20] Riley Booth and Peter Goldsmith. A wrist-worn piezoelectric sensor array for gesture input. *Journal of Medical and Biological Engineering*, 38(2):284–295, 2018.